INFN

Measurements of Carbon ion fragmentation on a thin Carbon target by the FIRST collaboration at GSI

Francesca Balestra – on behalf of the FIRST collaboration

Politecnico di Torino and INFN – Sezione di Torino

26-30/01/2015

Overview

INFN

Introduction
The FIRST experiment
Results
Conclusions and Outlook

Motivation of the FIRST experiment
State of the art of Particle Therapy and Space Radiation Protection

Why measurements of fragmentation cross sections?

INFN

3 fundamental applications:

- Particle Therapy
- Space Radiation Protection
- To improve the particle Transport Codes

Introduction
The FIRST experiment
Results
Conclusions and Outlook

Motivation of the FIRST experiment
State of the art of Particle Therapy and Space Radiation Protection

Experiments to study ^{12}C-^{12}C differential fragmentation cross sections for Particle Therapy and Space Radiation Protection applications

- Particle Therapy: for deep-seated tumors (depths up to ≈30 cm), it is necessary to explore the fragmentation processes in an energy range of 30-400 MeV/u

- Space Radiation Protection: Cosmic Rays are intensely energetic, hence to study their effects on human tissues is necessary to investigate an energy range of 100 MeV/u-10 GeV/u

Effects of nuclear fragmentation
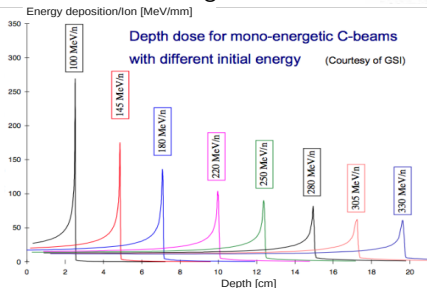
The greater is the penetration depth, the smaller is the peak-to-entrance dose ratio due to the diminishing of primary C ions

- Recently the scientific community is exploring the interesting region for therapeutic applications: e.g.
  - FRAG (LNS): C + C @ 62 & 80 MeV/u; M.De Napoli et al., PMB 57 7651, 2012
  - E600 (GANIL): C + (C, CH2, Al, Ti, PMMA) @ 95 MeV/u; J.Dudouet et al., Phys. Rev. C 88, 2013
  - FIRST (GSI): C+C @ 400 MeV/u; V.Patera et al., NIM A 678, 2012
  Discussed HERE. The results will be documented in a paper submitted to Phys. Rev. C

Introduction
The FIRST experiment
Results
Conclusions and Outlook

Motivation of the FIRST experiment
State of the art of Particle Therapy and Space Radiation Protection

Monte Carlo codes in Particle Therapy and Space Radiation Protection applications

- Particle transport codes are currently not able to fit the data (with the required accuracy, $< 3\%$ for Particle Therapy) in these fields
- As an example: from J. Dudouet et al., Phys. Rev. C 89, (2014)
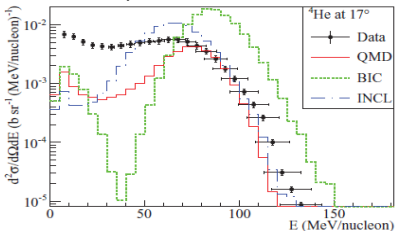
- Data: E600 (GANIL): C+C @ 95 MeV/u
- MC simulation: GEANT4

- The disagreements among the simulations and the data are due to the lack of information about the fragmentation processes
- This is due to the reduced number of experimental data available:
  - in particular, the double differential cross section for the fragmentation of carbon ions on thin targets at 400 MeV/u is missing!
  - other measurements done using carbon ions (like FRAG or E600) use different experimental conditions (beam energies, targets, emission angles)

Introduction
The FIRST experiment
Results
Conclusions and Outlook
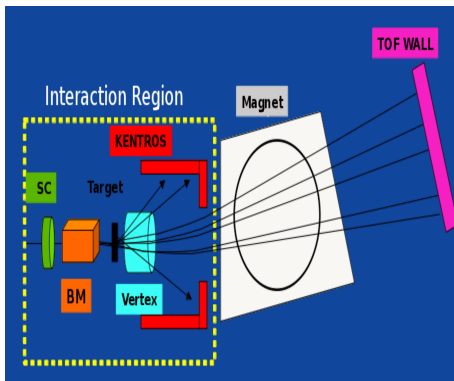
Data Taking
Experimental Setup
Analysis of Data

The experimental conditions

- FIRST (Fragmentation of Ions Relevant for Space and Therapy) is carried out by an international collaboration including different countries: France, Germany, Italy and Spain.

- The 1st data taking has been carried out with the following experimental conditions:
    - in the GSI laboratories (Darmstadt, Germany)
    - BEAM: ^{12}C @ 400 MeV/u, flux: 1-2 KHz
    - TARGETS: carbon and gold
        - $\approx 25 * 10^6$ ^{12}C ions passed through the carbon target
        - $\approx 5 * 10^6$ ^{12}C ions passed through the gold target

- The results illustrated here concern only:
    - the reaction: ^{12}C beam on ^{12}C target
    - the fragmentation at small polar angle: $\theta <$ 5 deg

- The results of the reaction ^{12}C beam on Au target and about the fragmentation at high polar angle will be illustrated in further presentations/publications

Introduction
The FIRST experiment
Results
Conclusions and Outlook

Data Taking
Experimental Setup
Analysis of Data

FIRST experiment layout

Features

- simultaneous tracking of several fragments
- particle identification based on energy deposition in ToF-Wall with the help of Vertex
- large angular acceptance of the whole detector assembly

- Start Counter SC: a scintillator to provide the trigger and the Start to the Time of Flight,
- Beam Monitor BM: a drift chamber to measure the beam trajectory and the impact point on the target,
- VERTEX VTX: a pixel silicon Detector (MIMOSA26), to track the fragments emerging from the target ($\theta :\leq 40 deg$; $\phi : 2\pi$) and to help in identifying the fragment charge,
- KENTROS: a thick scintillator to detect the light fragments (H, He) at large angle ($\theta >5$ deg),
- ALADiN: a magnet operating at a current of 680 A, to perform the evaluation of the fragment $\frac{p}{Z}$ ratio,
- ToF-Wall TW: a large area set of scintillators (2 planes) to measure the impinging point, the arrival time of the particles and the energy deposited inside the scintillators and therefore to perform the identification of the fragment charge.
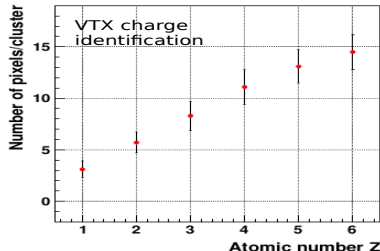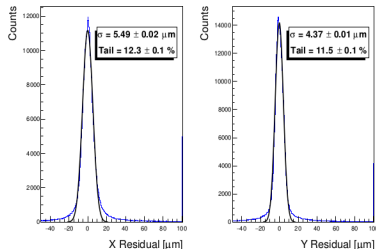
Introduction
The FIRST experiment
Results
Conclusions and Outlook

Data Taking
Experimental Setup
Analysis of Data

The VERTEX detector VTX

- Pixel Silicon Detector (4 planes) to track the fragments emerging from the target

X and Y resolutions
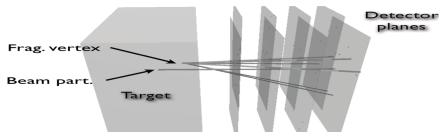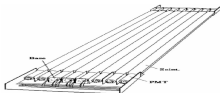

- Efficiency of fragment tracking:$\approx 99\%$
- Excellent tracking resolution $<10\mu m$ (x,y) and $<50\mu m$ (z)
- It can provide also information on the fragment charge: using the number of fired pixels per cluster
- The integration time (115 μs) of VTX can cause Pile-up (taken into account)
  - the BM is used to predict the impact point of the beam on the target. For piled-up events, the positions of the vertices reconstructed by VTX are compared with the position predicted by BM and the vertex closer to the BM is selected

Introduction
The FIRST experiment
Results
Conclusions and Outlook
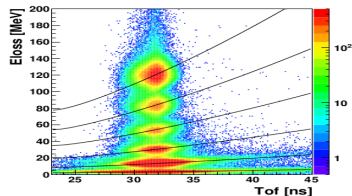
Data Taking
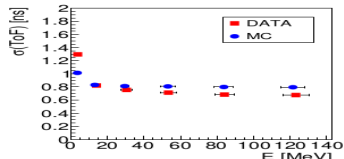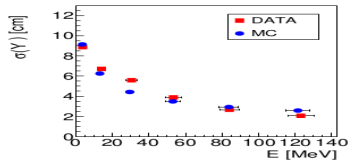Experimental Setup
Analysis of Data

The ToF-Wall detector TW

- 2 planes of scintillator of 96 slats each ($2.5 \times 1 \times 110$ cm^3)

- to measure the impinging point, the arrival time of the particles and the energy deposited inside the scintillators
  - to perform the identification of the fragment charge using an algorithm based on detected dE/dX in the TW vs ToF
- horizontal coordinate resolution X: deriving from the slat width $\frac{2.5}{\sqrt{12}} = 0.7$ cm
- vertical coordinate resolution Y: 2–5 cm
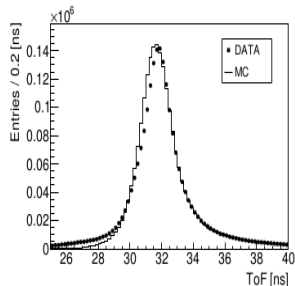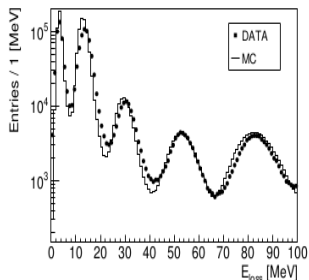- Time of Flight (ToF) resolution: $\approx$ 800 ps

Y and ToF resol. vs releas. energy

Introduction
The FIRST experiment
Results
Conclusions and Outlook

Data Taking
Experimental Setup
Analysis of Data

Data–MC comparisons
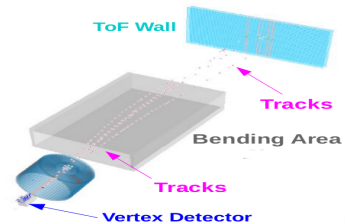
The simulation of the experiment is based on the general purpose Monte Carlo (MC) code FLUKA.

- The detailed MC simulation of the geometry and of the detector response is needed to evaluate the acceptances, the resolutions and the efficiencies for the cross section measurement

- The comparisons between the measured (by TW) and simulated Y, E_{loss} and ToF coordinates are shown

Introduction
The FIRST experiment
Results
Conclusions and Outlook

Data Taking
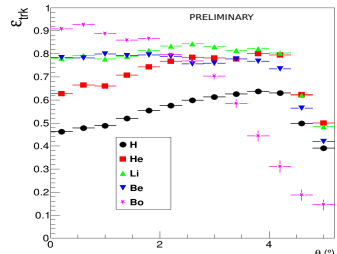Experimental Setup
Analysis of Data
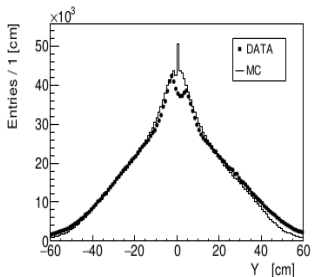
The Global Reconstruction Algorithm

- The Global Reconstruction is implemented to determine, for each fragment:
  - momentum $\vec{p} \Rightarrow E_k$
  - mass number A and charge Z
  - azimuthal ϕ and polar θ angles
- Based on the match among VTX tracks and TW hits
- Iterative forward-tracking of the VTX tracks through the magnetic field up to TW, by varying the momentum
- The tracking reconstruction efficiency ϵ_{trk} is defined as: $\epsilon_{trk} = \frac{n_{Rec}}{n_{Prod}}$
  - estimated using the full sample of the MC simulation (105 million of events)
  - n_{Prod} is the number of simulated charged fragments within the ALADiN acceptance
  - n_{Rec} is the number of properly reconstructed MC tracks

ToF Wall

Tracks

Bending Area

Tracks

Vertex Detector

e.g.: $\epsilon_{trk}(\theta)$ ranges within the 60%-90% for all the Z>1
(for protons, a lower ϵ_{trk} is expected)

Introduction
The FIRST experiment
Results
Conclusions and Outlook

Differential cross section in solid angle
Differential cross section in kinetic energy per nucleon
Comparison with other experiments

Evaluation of the differential cross sections

$$\frac{d\sigma^{Z,A}}{dE} = \frac{Y_i^{Z,A}}{N_{12_C} * N_{t,S} * \Delta E_i * \epsilon_{trk}(E_i)}$$

$$\frac{d\sigma^{Z,A}}{d\Omega} = \frac{X_j^{Z,A}}{N_{12_C} * N_{t,S} * \Delta\Omega_j * \epsilon_{trk}(\theta_j)}$$

$X_j^{Z,A}$ is the number of reconstructed fragments with charge Z and mass number A in the solid angle interval $\Delta\Omega_j = 2\pi\Delta(cos\theta_j)$
$\Delta(cos\theta_j)$ is the cosine interval corresponding to the polar angle interval $\Delta\theta_j$:
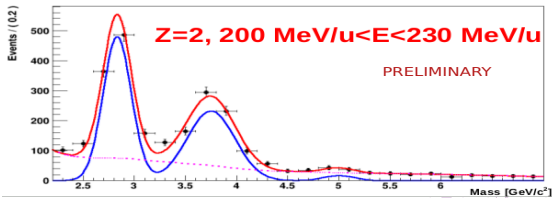$\Delta(cos\theta_j) = cos(\theta_j - \frac{\Delta\theta_j}{2}) - cos(\theta_j + \frac{\Delta\theta_j}{2})$

$Y_i^{Z,A}$ is the number of reconstructed fragments with charge Z and mass number A in the normalized kinetic energy (E_{kin}/n) interval ΔE_i

- N_{12_C} is the number of carbon ions impinging on the target: $24*10^6$
- $N_{t,S}$ is the surface nuclear density of the target: $\rho*t = 3.43$ g/cm^2
  (ρ is the target density, t is the target thickness)
- $\epsilon_{trk}(E)$ and $\epsilon_{trk}(\theta)$ are the tracking reconstruction efficiencies: $\epsilon_{trk} = \frac{n_{Rec}}{n_{Prod}}$

Introduction
The FIRST experiment
Results
Conclusions and Outlook

Differential cross section in solid angle
Differential cross section in kinetic energy per nucleon
Comparison with other experiments

Fragment yields measurements

- The mass spectra, obtained through the Global Reconstruction (GR), are fitted, for each charge and angular (energy) bin $\Delta\Omega$ (ΔE) to measure the fragment yield for each isotope
- The yields of signal and background are obtained (with uncertainties) using an unbinned extended maximum likelihood fit
- Signal (for each isotope) is modeled with a Gaussian signal Probability Density Function (PDF)
- Background PDFs take into account the combinatorial bkg:
  - wrong combination of VTX tracks with noise on TW
  - contribution of tracks/hits from real fragments badly associated by the GR
  - shape estimated on MC; normalization on DATA
- In addition, a "crossfeed" background due to real tracks/fragments with wrong charge ID has been considered (modeled with Gaussian PDF)

Introduction
The FIRST experiment
Results
Conclusions and Outlook

Differential cross section in solid angle
Differential cross section in kinetic energy per nucleon
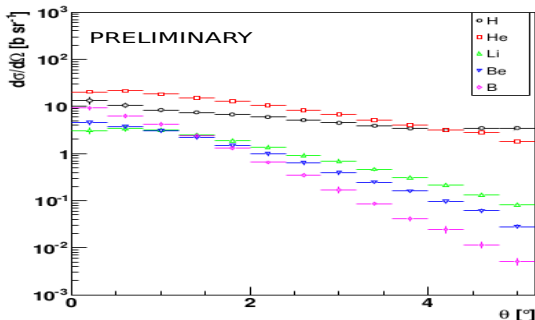Comparison with other experiments

The cross section results: the Single Differential Cross Sections $\frac{d\sigma^{Z,A}}{d\Omega}$

The angular differential cross sections, summed over all the isotopes,

$$\frac{d\sigma^Z}{d\Omega} \equiv \sum_A \frac{d\sigma^{Z,A}}{d\Omega}$$

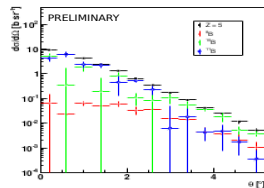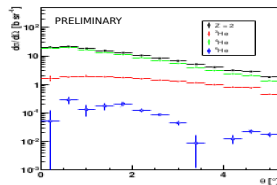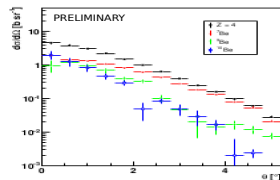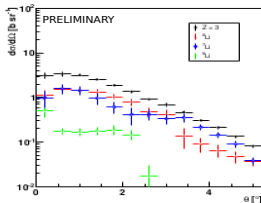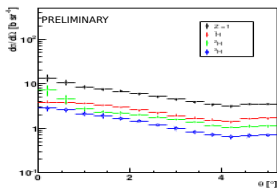are plotted as a function of the polar angle θ for each Z, in the following.

INFN

The heaviest fragments (Z=3,4,5) are more forwardly focused (nearly within 2 degrees) than H and He.
From the point of view of the energy loss (relevant for particle therapy) the heavier fragments release energy close to the trajectory of the primary beam.

Introduction
The FIRST experiment
Results
Conclusions and Outlook

Differential cross section in solid angle
Differential cross section in kinetic energy per nucleon
Comparison with other experiments

The cross section results: the Single Differential Cross Sections $\frac{d\sigma^{Z,A}}{d\Omega}$

Contribution of each single isotope of the charges Z=1,2,3,4,5 to $\frac{d\sigma^{Z,A}}{d\Omega}$

- the isotope production reflects the natural abundance
- α isotopes: most abundant

Introduction
The FIRST experiment
Results
Conclusions and Outlook

Differential cross section in solid angle
Differential cross section in kinetic energy per nucleon
Comparison with other experiments

The forward cross section

The forward cross section $\sigma^Z(\theta \leq 5deg)$ for the production of fragments with the same charge Z, in the angular range ($0 \leq \theta \leq 5$ deg) is obtained by summing up the contributions of all the isotopes and integrating in the θ range:

$$\sigma^Z(\theta \leq 5deg) \equiv 2\pi \int_{cos(\theta=5deg)}^1 \sum_A \frac{d\sigma^{Z,A}}{d\Omega} d(cos\theta)$$

These forward cross sections are listed in the table as a function of the charge Z

Z	$\sigma^Z(< 5°)$ [b]
1	0.11 (0.013)
2	0.15 (0.012)
3	0.021 (0.0037)
4	0.014 (0.0033)
5	0.014 (0.0065)

It is clearly visible that the forward direction ($0 \leq \theta \leq 5$ deg) is mostly populated by low charge fragments (Z=1,2): the fragmentation process emits forward protons, deuterons, tritons, ^{3}He and α particles nearly one order of magnitude more than isotopes of Li, Be and B.

Introduction
The FIRST experiment
Results
Conclusions and Outlook

Differential cross section in solid angle
Differential cross section in kinetic energy per nucleon
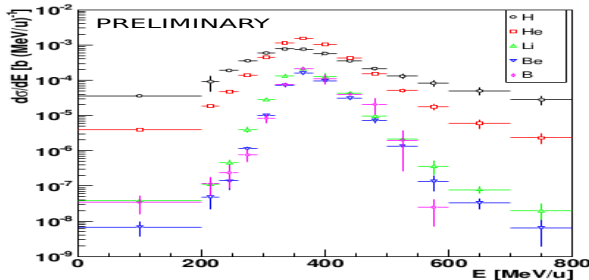Comparison with other experiments

The cross section results: the Single Differential Cross Sections $\frac{d\sigma^{Z,A}}{dE}$

The energy differential cross sections, summed over all the isotopes,

$$\frac{d\sigma^Z}{dE} \equiv \sum_A \frac{d\sigma^{Z,A}}{dE}$$

of each Z, are reported, vs the measured kinetic energy per nucleon.
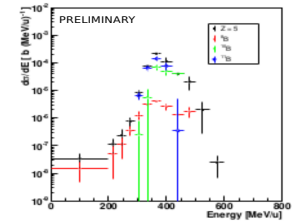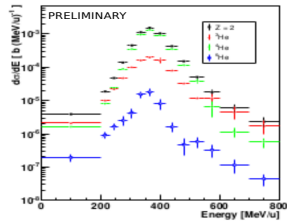

The kinetic energy distribution has not yet been unfolded to take into account the detector resolution

- the distributions of all the charges are bell-shaped in semilogarithmic scale
- the position of the peak of the distributions is, for all the charges, close to about 360 MeV/u: slightly lower than the primary beam (400 MeV/u)
- the highest charges (Z=3–5) are narrower distributed: residuals of ^{12}C beam (?)
- H and He ions cover a larger range in energy

Introduction
The FIRST experiment
Results
Conclusions and Outlook

Differential cross section in solid angle
Differential cross section in kinetic energy per nucleon
Comparison with other experiments

The cross section results: the Single Differential Cross Sections $\frac{d\sigma^{Z,A}}{dE}$

Contribution of each single isotope of the charges Z=1,2,3,4,5 to $\frac{d\sigma^{Z,A}}{dE}$
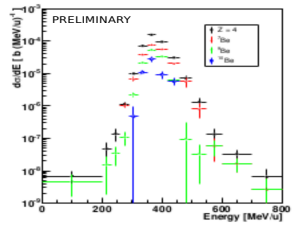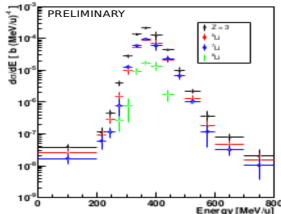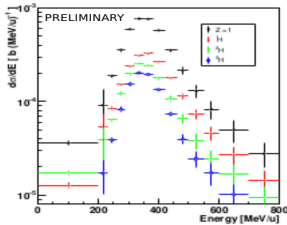
- the isotope production reflects the natural abundance
- α isotopes: most abundant

Introduction
The FIRST experiment
Results
Conclusions and Outlook

Differential cross section in solid angle
Differential cross section in kinetic energy per nucleon
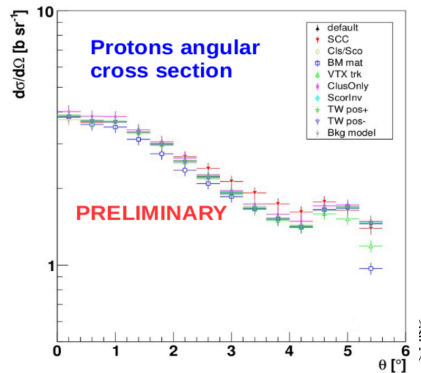Comparison with other experiments

The systematic errors

The measurements are dominated by systematic uncertainties.
How the systematic errors are evaluated?

- The analysis is repeated several times, changing the strategy, the algorithms, the corrections.
  In this way a systematic uncertainty is assigned.

Systematic checks:

- PDF modeling: the description of the BKG has been varied (modified shapes and different background contamination conditions)

- Variation of the thresholds for the fragment detection on TW: impact mainly on proton

- Tracking algorithms: changes in the L0 algorithm [VTX tracking, TW hit efficiency/clustering] and in the global algorithm [BM-VTX matching, scoring function weights] conditions.

- Detector description and alignment: global positioning of detectors (TW and ALADiN) has been varied within the precision achieved by the survey ($\pm$ 1 cm for the TW)

Protons angular cross section

PRELIMINARY

Introduction
The FIRST experiment
Results
Conclusions and Outlook

Differential cross section in solid angle
Differential cross section in kinetic energy per nucleon
Comparison with other experiments

400 MeV/u ^{12}C beams on elemental targets @ HIMAC, Zeitlin et al., 2007

- EXPERIMENT: experiments @ HIMAC (Zeitlin et al., Phys. Rev. C 76, 2007)
- REACTION: ^{12}C on ^{12}C @ 400 MeV/u (= FIRST)
- APPARATUS: Si detectors

INFN

COMPARISON WITH FIRST: ANGULAR DISTRIBUTION vs Z

Fragment Charge Z	$d\sigma/d\Omega$ (b/sr) FIRST $\theta=5°$ STAT ERR ONLY	$d\sigma/d\Omega$ (b/sr) @ HIMAC $\theta=5°$
	$1°<\theta<5°$	$\theta=5°\pm3.9°$
1	4.89 ± 0.08	7.63 ± 0.23
2	6.42 ± 0.12	4.22 ± 0.13
3	0.771 ± 0.017	0.20 ± 0.01
4	0.580 ± 0.014	0.054 ± 0.005

× differences in the angular acceptances:
FIRST: $\Delta\Omega=4*10^{-3}$ sr; @ HIMAC: $\Delta\Omega=14*10^{-3}$ sr $\Rightarrow$ difficult comparison

✓ even if in different experimental conditions, the order of magnitude of the cross sections is the same in the two experiments

Introduction
The FIRST experiment
Results
Conclusions and Outlook

Differential cross section in solid angle
Differential cross section in kinetic energy per nucleon
Comparison with other experiments

E600: 95 MeV/u ^{12}C beams on thin targets @ GANIL, Dudouet et al, 2013

- EXPERIMENT: E600 (J.Dudouet et al., Phys. Rev. C 88, 2013)
- REACTION: ^{12}C on ^{12}C @ 95 MeV/u (< FIRST)
- APPARATUS: 4 ΔEthin/ΔEthick/E telescopes

COMPARISON WITH FIRST: ENERGY DISTRIBUTIONS
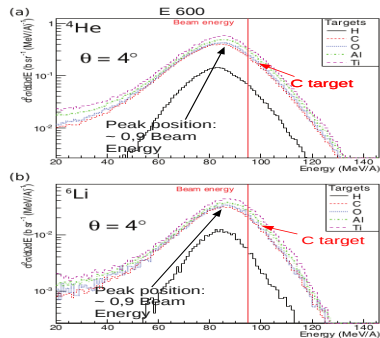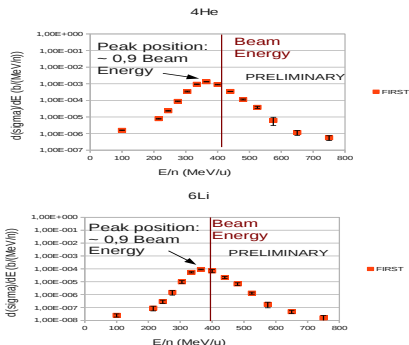
In semilogarithmic scale:
- ✓ the energy distribution is bell-shaped for both the experiments
- ✓ the distributions show a similar trend also for the shape of tails
- ✓ the distribution peak is around 0.9 of the beam energy for both the experiments
- ✓ also for the E600 experiment, heavier ions have a distribution in energy narrower than light ions

Conclusions

- FIRST performed measurements of fragmentation cross sections, as a function of emission angles and kinetic energies of the fragments and produced a data sample of several million collisions of ^{12}C ions impinging on a C target.
  These measurements fulfill a serious gap in the previous data concerning the differential cross section of fragmentation of carbon ions at 400 MeV/u.

- The plots of the single differential cross sections pointed out important preliminary outcomes.
  - Polar angle distributions:
    - Z= 1-2: spread out over the 0-5 deg angular range $\Rightarrow$ contribute to the dose scattering far from the original beam direction
    - Z= 3-5: emitted at smaller angles ($\lesssim$ 2 deg) $\Rightarrow$ contribute to the dose deposition close to the primary beam trajectory
  - Kinetic energy distributions:
    - Distributions are dominated by a bell-shaped peak centered close to the beam energy per nucleon (400 MeV/u)

- The results illustrated here will be documented in a paper submitted to Phys. Rev. C

Conclusions and Outlook

Comparison with data from the most recent experiments:
@ HIMAC (Zeitlin et al., 2007); E600 (2013)

- @ HIMAC: the order of magnitude for the angular differential cross section is the same, even if the angular acceptance is different
- E600: energy distributions have similar trends, even if at different energy

OUTLOOK

- To complete the data analysis in order to achieve results also in the angular range $\theta > 5$ deg, for the C target
- To perform the analysis of the data collected on the Au target
- To perform a refinement of the data analysis in order to obtain the Double Differential Cross Sections (DDCS) $\frac{d^2\sigma}{d\Omega dE}$, for each fragment type

THE END

Thanks for your attention

INFN